JOC Article

Effects of Fluorine on the Structures and Energetics of the Propynyl and Propargyl Radicals and Their Anions

Raj K. Sreeruttun,[†,‡] Ponnadurai Ramasami,*[,†] Chaitanya S. Wannere,[‡] Ankan Paul,[‡] Paul v. R. Schleyer,[‡] and Henry F. Schaefer III*[,‡]

Department of Chemistry, University of Mauritius, Réduit, Mauritius, and Center for Computational Chemistry, University of Georgia, Athens, Georgia 30602

hfs@uga.edu; p.ramasami@uom.ac.mu

Received April 15, 2005

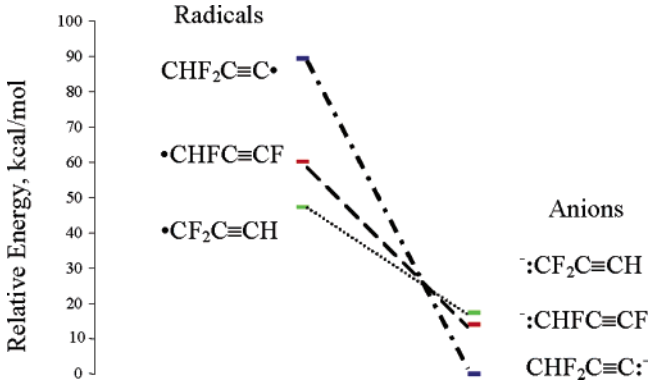

The adiabatic electron affinity (EA_{ad}) of the $CH_3-C\equiv C^\bullet$ radical [experiment = 2.718 ± 0.008 eV] and the gas-phase basicity of the $CH_3-C\equiv C:^-$ anion [experiment = 373.4 ± 2 kcal/mol] have been compared with those of their fluorine derivatives. The latter are studied using theoretical methods. It is found that there are large effects on the electron affinities and gas-phase basicities as the H atoms of the α-CH_3 group in the propynyl system are substituted by F atoms. The predicted electron affinities are 3.31 eV ($FCH_2-C\equiv C^\bullet$), 3.86 eV ($F_2CH-C\equiv C^\bullet$), and 4.24 eV ($F_3C-C\equiv C^\bullet$), and the predicted gas-phase basicities of the fluorocarbanion derivatives are 366.4 kcal/mol ($FCH_2-C\equiv C:^-$), 356.6 kcal/mol ($F_2CH-C\equiv C:^-$), and 349.8 kcal/mol ($F_3C-C\equiv C:^-$). It is concluded that the electron affinities of fluoropropynyl radicals increase and the gas-phase basicities decrease as F atoms sequentially replace H atoms of the α-CH_3 in the propynyl system. The propargyl radicals, lower in energy than the isomeric propynyl radicals, are also examined and their electron affinities are predicted to be 0.98 eV ($^\bullet CH_2-C\equiv CH$), 1.18 eV ($^\bullet CFH-C\equiv CH$), 1.32 eV ($^\bullet CF_2-C\equiv CH$), 1.71 eV ($^\bullet CH_2-C\equiv CF$), 2.05 eV ($^\bullet CFH-C\equiv CF$), and 2.23 eV ($^\bullet CF_2-C\equiv CF$).

I. Introduction

Free radicals and anions incorporating (terminal) C≡C triple bonds (e.g. $H-C\equiv C^\bullet$, $H(C\equiv C)_n-C\equiv C^\bullet$, $Ph-C\equiv C^\bullet$, $R-C\equiv C^\bullet$, etc., and their respective anions) are accepted constituents of combustion, atmospheric chemistry, and even interstellar chemistry.[1] These molecules have captured experimental and theoretical attention in part due to their high enthalpies of formation.[2] The substituted ethynyl anions in metal acetylides[3] have been used preferentially in the synthesis of inorganic complexes[4] as well as in some interesting polymerization techniques.[5] Metal acetylides have been increasingly exploited in the molecular design of luminescent metal-based materials.[6]

[†] University of Mauritius
[‡] University of Georgia

(1) (a) Lovas, F. J.; McMahon, R. J.; Grabow, J.-U.; Schnell, M.; Mack, J.; Scott L. T.; Kuczkowski, R. L. *J. Am. Chem. Soc.* **2005**, *127*, 4345 and references therein. (b) McCarthy, M. C.; Chen, W.; Apponi, A. J.; Gottlieb, C. A.; Thaddeus, P. *Astrophys. J.* **1999,** *520*, 158.

(2) Wodtke, A. M.; Lee, Y. T. *J. Phys. Chem.* **1985**, *89*, 4744.

(3) (a) Tedeschi, C.; Saccavini, C.; Maurette, L.; Soleilhavoup, M.; Chauvin, R. *J. Organomet. Chem.* **2003**, *670*, 151. (b) Goldfuss, B.; Schleyer, P. v. R.; Hampel, F. *J. Am. Chem. Soc.* **1997**, *119*, 1072.

(4) (a) Briggs, T. F.; Winemiller, M. D.; Xiang, B.; Collum, D. B. *J. Org. Chem.* **2001**, *66*, 6291. (b) Crescenzl, R.; Sterzo, C. L. *Organometallics* **1992**, *11*, 4301.

(5) (a) Zhang, W.; Moore, J. S. *J. Am. Chem. Soc.* **2004**, *126*, 12796. (b) Brisdon, A. K.; Crossley, I. R.; Pritchard, R. G.; Sadiq G.; Warren, J. E. *Organometallics* **2003**, *22*, 5534. (c) Fürstner, A.; Guth, O.; Rumbo A.; Seidel, G. *J. Am. Chem. Soc.* **1999**, *121*, 11108.

10.1021/jo0507688 CCC: $30.25
Published on Web 09/24/2005

Considerable experimental and theoretical effort has been devoted to the study of the molecular structures of α-fluoropropyne[7−9] and α-trifluoropropyne.[10] Theoretical studies have been performed to predict the acidity of the acetylenic proton and the homolytic bond dissociation enthalpies of the C−H bond adjacent to the α-CF_3 group of the fluorine derivatives of propyne.[11] Further, experimental investigations, such as liquid-phase Raman spectra and solution-phase infrared spectra,[8] have also been reported for α-fluoropropyne. In a recent study of the α-trifluoropropyne, Chirakul and Sigurdsson observed that this alkyne unexpectedly adds to 2′-deoxy-5-iodouridine through a Michael type addition.[12]

Various experimental and theoretical advances in chemistry have been applied to derivatives of α-fluoropropyne, also called propargyl fluoride.[13] However, there have been fewer studies pertaining to fluoropropynyl radicals and their anions. Thus, the present research aims at determining the electron affinities of the fluorine derivatives of the propynyl radical ($F_nCH_{3-n}-C\equiv C^{\bullet}$, n = 1−3) and their isomeric propargyl fluorides. Further, this work also focuses on the gas-phase basicities of the fluorine derivatives of the propynyl anion ($F_nCH_{3-n}-C\equiv C:^{-}$, n = 1−3). Experimentally, the electron affinity of the $CH_3-C\equiv C^{\bullet}$ radical has been measured by Robinson, Polak, Bierbaum, Depuy, and Lineberger to be 2.718 ± 0.008 eV.[14] Recent DFT studies with diffuse basis sets have shown that the propynyl electron affinity (EA) predicted at the B3LYP/DZP++ level of theory is in close agreement with this experimental value.[15]

This research compares the known electron affinity of the $CH_3-C\equiv C^{\bullet}$ radical with those of its fluorine derivatives. One expects to observe significant EA changes as the electron-withdrawing fluorines sequentially substitute each H atom of the α-CH_3 group of the propynyl system.[16] The geometries of these fluorine-substituted radicals and their electronic structures have been investigated here. Moreover, the gas-phase basicities of the three different fluoropropynyl anionic species have also been studied and compared with the limited available experimental data.

In acetylene chemistry, lithium-based compounds such as lithium acetylides have great importance, especially in the synthesis of new C−C σ bonds and the incorporation of the C≡C linkage in parent molecules.[17] Finally, this research investigates the lithium fluoropropyne(s) ($F_nCH_{3-n}-C\equiv C:^{-}$ Li^{+}, n = 1−3) in an attempt to study their stabilities with respect to the free propynyl species in the gas-phase.

II. Theoretical Methods

All theoretical computations were performed with the Gaussian 94 suite of programs.[18] Density functional theory (DFT) has been used to investigate the total energies, equilibrium energies, vibrational frequencies, adiabatic electron affinities, and ZPVE-corrected electron affinities of the fluoropropynyl systems using a double-ζ basis set with polarization and diffuse function, denoted as DZP++. The different gradient-corrected density functional methods used are BHLYP, BLYP, B3LYP, BP86, BPW91, and B3PW91.[19−23] The double-ζ basis sets were constructed by augmenting the Huzinaga−Dunning−Hay[24−26] sets of contracted Gaussian functions with one set of p polarization functions for each H atom, one set of d polarization functions for each C and each F atom, respectively, and one set of p polarization functions of lithium atom [$\alpha_p(H) = 0.75$, $\alpha_d(C) = 0.75$, $\alpha_d(F) = 1.0$, and $\alpha_p(Li) = 0.0205$]. These basis sets were further augmented with diffuse functions. Diffuse functions were determined in an even-tempered fashion according to the prescription of Lee and Schaefer,[27]

$$\alpha_{\text{diffuse}} = \left(\frac{\alpha_1}{\alpha_2} + \frac{\alpha_2}{\alpha_3}\right)\alpha_1$$

where α_1, α_2, and α_3 are the three smallest Gaussian orbital exponents of the s- or p-type primitive functions of a given atom ($\alpha_1 < \alpha_2 < \alpha_3$) [$\alpha_s(H) = 0.04415$, $\alpha_s(C) = 0.04302$, $\alpha_p(C) = 0.03629$, $\alpha_s(F) = 0.1049$, $\alpha_p(F) = 0.0826$, $\alpha_s(Li) = 0.00717523$, and $\alpha_p(Li) = 0.00713759$]. The final contraction scheme is as follows: H (5s1p/3s1p), C(10s6p1d/5s3p1d), F(10s6p1d/5s3p1d), and Li(10s5p1d/5s3p1d).

The fluoropropynyl equilibrium geometries were optimized using analytic energy gradients for each DFT functional, and the optimization processes were conducted under tight convergence criteria. The integrals determined analytically were evaluated with an accuracy of 10 digits, and the density was converged to 10^{-8}. The default-pruned grid in Gaussian 94 consisting of 75 radial shells with 302 angular points per shell was used for the numerical integrations.

Two different radical-anion energy differences were predicted from total energies. The adiabatic and ZPVE-corrected electron affinities are given as follows:

Adiabatic electron affinity, EA_{ad} =

$$E(\text{optimized radical}) - E(\text{optimized anion})$$

(6) Yam, V. W.-W. *Pure Appl. Chem.* **2001**, *73*, 543.
(7) Honjou, N. *J. Phys. Chem.* **1988**, *92*, 2410.
(8) Douglass, K. O.; Rees, F. S.; Suenram, R. D.; Pate, B. H.; Leonov, I. *J. Mol. Spectrosc.* **2005**, *230*, 62.
(9) Wiedenmann, K. H.; Botskor, I.; Rudolph, H. D. *J. Mol. Spectrosc.* **1985**, *113*, 186.
(10) Okabe, H.; Cody, R. J.; Allen, J. E. *Chem. Phys.* **1985**, *92*, 67.
(11) (a) Zhang, X.-M. *J. Org. Chem.* **1998**, *63*, 3590. (b) Powell, M. F.; Peterson M. R.; Csizmadia, I. G. *J. Mol. Struct.* **1983**, *92*, 323.
(12) Chirakul P.; Sigurdsson, S. Th. *Tetrahedron Lett.* **2003**, *44*, 6899.
(13) (a) Prakesch, M.; Grée, D.; Grée, R. *Acc. Chem. Res.* **2002**, *35*, 175. (b) Hopkinson, A. C.; Lien, M. H. *J. Am. Chem. Soc.* **1986**, *108*, 2843. (c) Dorado, M.; Mó, O.; Yáñez, M. *J. Am. Chem. Soc.* **1980**, *102*, 947.
(14) Robinson, M. S.; Polak, M. L.; Bierbaum, V. M.; Depuy, C. H.; Lineberger, W. C. *J. Am. Chem. Soc.* **1995**, *117*, 6766.
(15) Sreeruttun, R. K.; Ramasami, P.; Yan, G.; Wannere, C. S.; Schleyer, P. v. R.; Schaefer, H. F. *Int. J. Mass Spectrom.* **2005**, *241*, 295.
(16) Chambers, R. D. *Fluorine in Organic Chemistry*; Blackwell: Oxford, 2004.
(17) Konno, T.; Chae, J.; Kanda, M.; Nagai, G.; Tamura, K.; Ishihara K.; Yamanaka, H. *Tetrahedron* **2003**, *59*, 7571.
(18) Frisch, M. J.; Trucks, G. W.; Schlegel, H. B.; Gill, P. M. W.; Johnson, B. G.; Robb, M. A.; Cheeseman, J. R.; Raghavachari, K.; Al-Laham, M. A.; Zakrzewski, V. G.; Ortiz, J. V.; Foresman, J. B.; Cioslwoski, J.; Stefanov, B. B.; Nanayakkaya, A.; Challacombe, M.; Peng, C. Y.; Ayala, P. Y.; Chen, W.; Wong, M. W.; Andres, J. L.; Replogle, E. S.; Gomperts, R.; Martin, R. L.; Fox, D. J.; Binkley, J. S.; Defrees, D. J.; Baker, J.; Stewart, J. P.; Head-Gordon, M.; Gonzalez, C.; Pople, J. A. *Gaussian 94*, Revision D. 4, Gaussian Inc: Pittsburgh, PA, 1995.
(19) Becke, A. D. *J. Chem. Phys.* **1993**, *98*, 1372.
(20) Lee, C.; Yang, W.; Parr, R. G. *Phys. Rev. B* **1988**, *37*, 785.
(21) Becke, A. D. *J. Chem. Phys.* **1993**, *98*, 5648.
(22) Perdew, J. P.; Chevary, J. A.; Vosko, S. H.; Jackson, K. A.; Pederson, M. R.; Singh, D. J.; Fiolhais, C. *Phys. Rev. B* **1993**, *48*, 4978.
(23) Perdew, J. P. *Phys. Rev. B* **1986**, *33*, 8822.
(24) Huzinaga, S. *J. Chem. Phys.* **1965**, *42*, 1293.
(25) Dunning T. H.; Hay, P. J. In *Modern Theoretical Chemistry*; Schaefer, H. F., Ed.; Plenum: New York, 1977; Vol. 3, pp 1−27.
(26) Huzinaga, S. *Approximate Atomic Wavefunctions II*; University of Alberta: Edmonton, Alberta, 1971.
(27) Lee, T. J.; Schaefer, H. F. *J. Chem. Phys.* **1985**, *83*, 1784.

ZPVE-corrected electron affinity =
$$[E(\text{optimized radical}) + \text{ZPVE}_{\text{radical}}] - [E(\text{optimized anion}) + \text{ZPVE}_{\text{anion}}]$$

The free energies were evaluated at the BHLYP, BLYP, B3LYP, BP86, BPW91, and B3PW91 levels with the DZP++ basis set following the frequency and zero-point energy computation as implemented in the Gaussian 94 program. The gas-phase basicities have the opposite sign of the Gibbs free-energy (ΔG) change associated with the reaction:

$$R{-}C{\equiv}C{:}^-_{(g)} + H^+_{(g)} \rightarrow R{-}C{\equiv}C{-}H_{(g)}$$

The C−H bond dissociation energies (homolytic cleavage) of fluoropropynes are also computed to compare with the gas-phase basicities (heterolytic CH bond breaking) as follows:

$$R{-}C{\equiv}C^{\bullet} + H^{\bullet} \rightarrow R{-}C{\equiv}C{-}H$$

In fact, the gas-phase basicity is the negative intrinsic acidity of a molecule. This research reports each gas-phase basicity of the fluoropropynyl anions as the difference in the sum of electronic and thermal free energies of the anion and the neutral species, as well as the thermal correction to the Gibbs free energy.

Ab initio techniques such as the Moller−Plesset perturbation theory (MP2) and the coupled-cluster singles, doubles, and noniterative triples corrections CCSD(T) have been applied to the fluoropropynyl systems. Specifically, single-point computations have been done with the CCSD(T)/DZP++ method at the MP2/DZP++ optimized geometries. In general, MP2 equilibrium geometries are expected to be of comparable reliability to B3LYP. However, few studies have concluded that structures optimized using ab initio methods may differ remarkably from those given by the DFT levels.[28] In addition, electron affinities predicted with MP2 are generally inferior to the best DFT predictions.[29]

III. Results and Discussion

Selected equilibrium geometries predicted with various DFT methods for the radicals and their respective anions are presented in Figures 1−6. All the radical species in this work have doublet electronic ground states, while the closed-shell anion species have singlet ground electronic states.

A. Σ and Π Radicals. A number of the systems examined here have Σ and Π electronic states that are nearly degenerate. Some discussion of the parent C_2H radical is appropriate in this context. The ground electronic state of the C_2H radical has $^2\Sigma^+$ symmetry. The spectroscopy of the C_2H radical has been the subject of important experimental studies. Most importantly for our purposes is the experimental value[30] of the $\tilde{X}\ ^2\Sigma^+ - \tilde{A}\ ^2\Pi$ band origin, T_o = 3692 cm^{-1} = 10.6 kcal/mol. The methods used in this research predict the following $^2\Sigma^+ - {}^2\Pi$ energy differences (in kcal/mol) for the C_2H radical: 2.1 (BHLYP), 8.0 (BLYP), 5.8 (B3LYP), 8.9 (BP86), 9.4 (BPW91), and 5.5 (B3PW91). Thus we see that the present DFT methods underestimate the $\tilde{X}\ ^2\Sigma^+ - \tilde{A}\ ^2\Pi$ energy separation in C_2H. This probably means that for the C_2R systems the DFT levels employed in this study underestimate the energy difference between the $^2\Sigma^+$ and $^2\Pi$ states. However, we only considered the $^2\Sigma^+$ states in the following discussion.

B. Monofluoropropynyl Radical and Anion. The $FCH_2{-}C{\equiv}C^{\bullet}$ radical (^{2}A), with C_1 symmetry, is predicted to have a CCCF dihedral angle (Ø) of 100.7° and a C−C≡C angle of 162.4°. The C_s geometry is not a genuine minimum on the potential energy surface for this radical at most of the DFT levels, but it is at MP2. The B3LYP/DZP++ method predicts the C_s radical to be a transition state with an imaginary frequency of 632i cm^{-1}. However, the MP2/DZP++ method does predict the C_s $FCH_2{-}C{\equiv}C^{\bullet}$ radical (^{2}A′) to be a minimum (lowest harmonic vibrational frequency = 245 cm^{-1}).

Similarly, the $FCH_2{-}C{\equiv}C{:}^-$ anion (^{1}A) optimizes to C_1 geometry, with the C−C≡C angle bending to 175.1°, and the CCCF dihedral angle close to 180°. However, the MP2/DZP++ method predicts that this anion has a C_s structure (^{1}A′) where the C−C≡C subunit is nearly linear. The optimized geometries for the monofluoropropynyl radical (on the left-hand side) and anion (right) are shown in Figure 1. From the microwave study of α-fluoropropyne ($FCH_2{-}C{\equiv}CH$),[9] the C−C≡C bond angle has been reported to be nearly linear, 178.9°. The B3LYP/DZP++ prediction for this closed-shell species shows a similar bending of 178.0° for the C−C≡C angle. Experimental bond lengths for α-fluoropropyne ($FCH_2C{\equiv}CH$) are C≡C = 1.206(4) Å, C−C = 1.454(4) Å, C−H = 1.096(2) Å, and C−F = 1.393(6) Å. The present B3LYP results for this neutral closed-shell species are C≡C = 1.214 Å, C−C = 1.468 Å, C−H = 1.098 Å, and C−F = 1.398 Å. In contrast, a significant degree of in-plane bending is predicted for the radical.

C. Difluoropropynyl Radical and Anion. Both the $F_2CH{-}C{\equiv}C^{\bullet}$ radical (^{2}A′) and the $F_2CH{-}C{\equiv}C{:}^-$ anion (^{1}A′) are predicted to have C_s structures. However, there is some bending of the C−C≡C frame in both the radical and its anion. For example, the B3LYP method predicts a bending angle of 158.9° for the radical, whereas for the anion, the C−C≡C angle is slightly bent, to 173.5°. However, the MP2 method predicts a nearly linear C−C≡C arrangement for both the radical and the anion. Figure 2 compares the optimized structures of the difluoropropynyl radical (left) and its anion (right).

D. Trifluoropropynyl Radical and Anion. The BHLYP, B3LYP, and B3PW91 methods predict C_{3v} geometries for both the $F_3C{-}C{\equiv}C^{\bullet}$ radical ($^2A_1$) and the $F_3C{-}C{\equiv}C{:}^-$ anion ($^1A_1$). However, the other functionals show a preference for C_s symmetry, causing the C−C≡C angle in the $F_3C{-}C{\equiv}C^{\bullet}$ radical to bend to approximately 160°, keeping the dihedral angle of the CCCF plane at 180°. The MP2 method favors a C_{3v} symmetry for both the radical and the anion. Figure 3 shows the optimized geometries of the trifluoropropynyl radical and anion, respectively.

E. Monofluoropropyne, Difluoropropyne, and Trifluoropropyne. The geometries of the neutral fluoropropynes are displayed in Figure 4 to offer a comparison with their radical and anion counterparts. The C≡C separations in the fluoropropynes fall in the range of 1.210−1.214 Å and are typical of alkyne bond lengths. Unlike the analogous radicals and anions, the equilibrium geometries of these structures are insensitive to the

(28) Plattner, D. A.; Houk, K. N. *J. Am. Chem. Soc.* **1995**, *117*, 4405. Pomerantz, A. E.; Han, J. H.; Musgrave, C. B. *J. Phys. Chem. A* **2004**, *108*, 4030.

(29) Rienstra-Kiracofe, J. C.; Tschumper, G. S.; Schaefer, H. F.; Nandi, S.; Ellison, G. B. *Chem. Rev.* **2002**, *102*, 231.

(30) Curl, R. F.; Carrick, P. G.; Merer, A. J. *J. Chem. Phys.* **1985**, *82*, 3479.

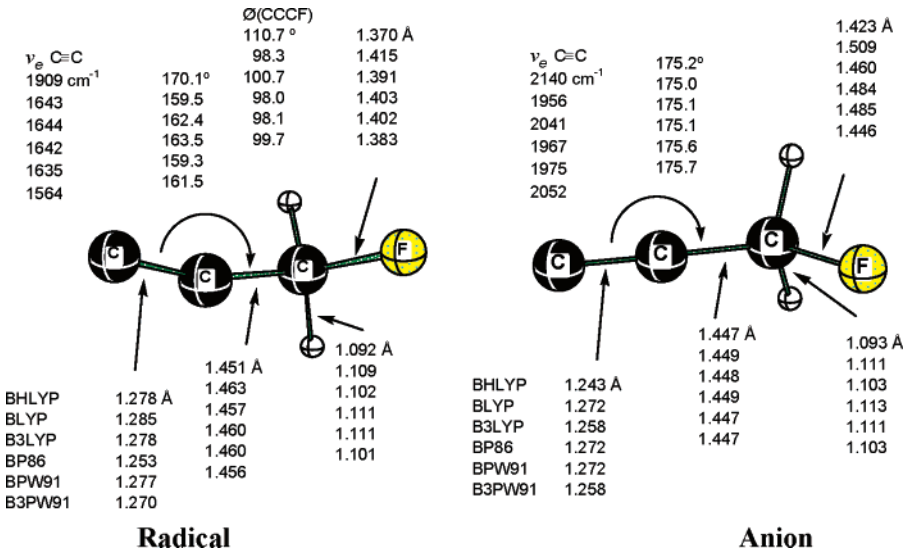

FIGURE 1. Optimized geometries for the α-fluoropropynyl radical (C_1, ^{2}A) and the α-fluoropropynyl anion (C_1, ^{1}A).

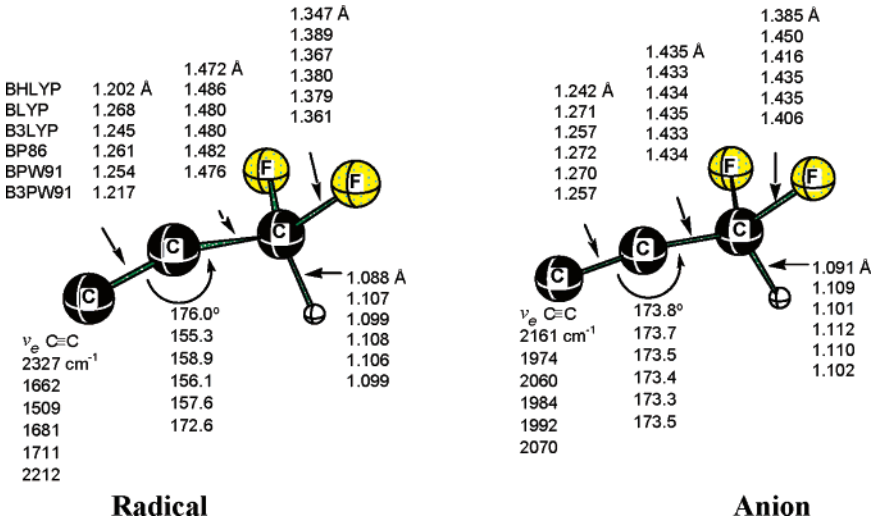

FIGURE 2. Optimized geometries for the α-difluoropropynyl radical (C_s, ^{2}A′) and the α-difluoropropynyl anion (C_s, ^{1}A′).

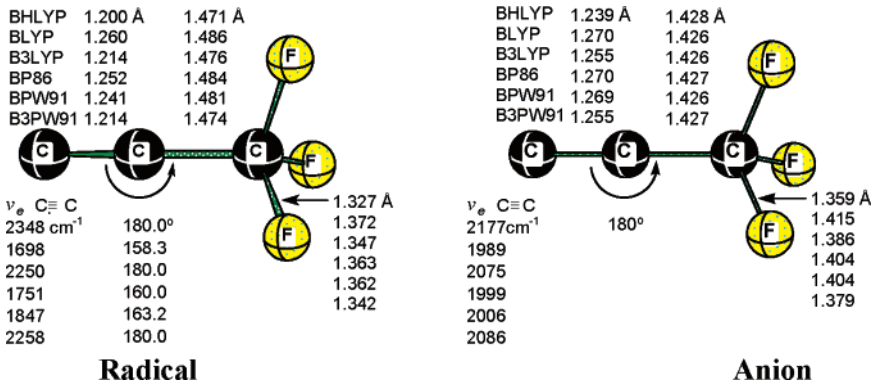

FIGURE 3. Optimized geometries for the α-trifluoropropynyl radical (C_{3v}, ^{2}A$_1$) and the α-trifluoropropynyl anion (C_{3v}, ^{1}A$_1$).

level of theory used; hence, we have reported geometries only from the B3LYP/DZP++ level. Note that C−C≡C subunits are nearly linear. Moreover the CC vibrational frequency is approximately 2200 cm^{-1}, typical for a CC triple bond, and does not change significantly with the level of theory used for optimization.

F. Lithium Fluoropropynes. Figure 5 shows the predicted structures for the lithium acetylides for the three fluorine derivatives of propyne at the B3LYP/DZP++ level of theory. The lithium fluoropropynides have linear or very nearly linear C−C≡C structures, which are very different from those of the free fluoro-

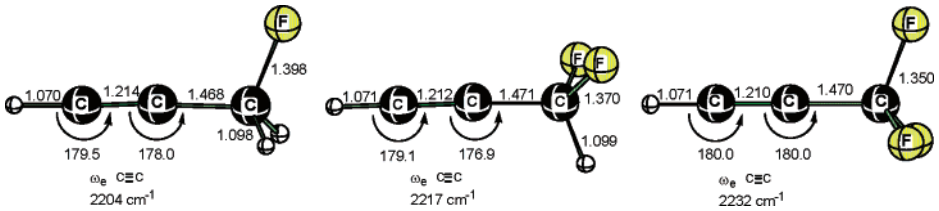

FIGURE 4. The B3LYP/DZP++ optimized geometries for monofluoropropyne (extreme left), difluoropropyne (middle), and trifluoropropyne (extreme right).

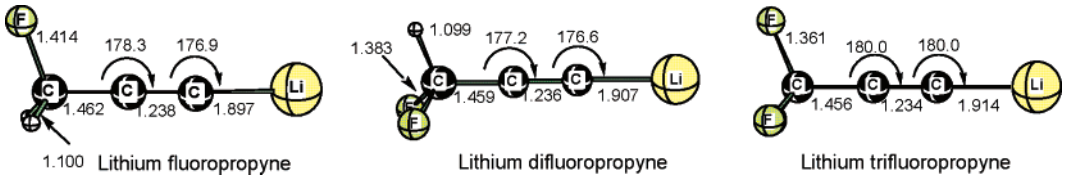

FIGURE 5. The B3LYP/DZP++ optimized geometries for the lithium fluoropropynes, $F_nCH_{3-n}C{\equiv}C{-}Li$.

TABLE 1. Theoretical Adiabatic Electron Affinities for the Fluoropropynyl Radicals[a]

		electron affinities (eV)			
methods		$CH_3{-}C{\equiv}C^{\bullet}$	$FCH_2{-}C{\equiv}C^{\bullet}$	$F_2CH{-}C{\equiv}C^{\bullet}$	$F_3C{-}C{\equiv}C^{\bullet}$
DFT	BHLYP/DZP++	2.60 (2.62)	3.09 (3.07)	3.62 (3.66)	3.95 (3.99)
	BLYP/DZP++	2.57 (2.55)	3.18 (3.18)	3.75 (3.75)	4.10 (4.10)
	B3LYP/DZP++	2.72 (2.70)	3.32 (3.31)	3.88 (3.86)	4.22 (4.24)
	BP86/DZP++	2.74 (2.73)	3.47 (3.32)	3.90 (3.90)	4.22 (4.22)
	BPW91/DZP++	2.60 (2.58)	3.19 (3.18)	3.72 (3.72)	4.06 (4.06)
	B3PW91/DZP++	2.67 (2.64)	3.25 (3.23)	3.74 (3.77)	4.06 (4.09)
ab initio	MP2/DZP++	2.96	3.58	4.05	4.39
	MP3DZP++//MP2/DZP++	2.70	3.28	3.73	4.07
	CCSD/DZP++//MP2/DZP++	2.41	2.97	3.39	3.72
	CCSD(T)/DZP++//MP2/DZP++	2.52	3.09	3.53	3.85
experiment	negative ion photoelectron spectroscopy	2.718 ± 0.008[b]			

[a] ZPVE-corrected electron affinities (eV) are in parentheses. [b] Reference 14.

propynyl radicals. Thus, the floppiness of the C−C≡C angle in the presence of the metal is insignificant.

G. Electron Affinities and Gas-Phase Basicities. The adiabatic and ZPVE-corrected electron affinities of the fluoropropynyl radicals are summarized in Table 1. The trend is clear: the electron affinity values for these radicals increase monotonically as the number of substituted fluorine atoms increases. Figure 8 shows that there is a nearly linear increase in the electron binding energies for the $CH_3{-}C{\equiv}C^{\bullet}$, $FCH_2{-}C{\equiv}C^{\bullet}$, and $F_2CH{-}C{\equiv}C^{\bullet}$ radicals. However, $F_3C{-}C{\equiv}C^{\bullet}$ deviates somewhat from this nearly linear behavior; its electron affinity is slightly smaller than expected from the correlation. A linearity for EA is expected for the $CH_3{-}C{\equiv}C^{\bullet}$, $FCH_2{-}C{\equiv}C^{\bullet}$, and $F_2CH{-}C{\equiv}C^{\bullet}$ radicals because (as discussed later in section I) the extra electron in the respective anions occupies the π-orbital, which is stabilized by the C−F σ^*-orbital. Thus the quantitative pictures of the radical SOMOs and their respective anion HOMOs are almost the same. However, a different behavior is expected (also seen in Figure 8) for the EA of the $F_3C{-}C{\equiv}C^{\bullet}$ radical because the extra electron in the anion now occupies the σ-bonding orbital.

The present B3LYP predictions show good agreement with the limited available experimental data. However, coupled-cluster computations underestimate the EA value for the $CH_3{-}C{\equiv}C^{\bullet}$ radical while the MP2/DZP++ method (2.96 eV) overshoots it (see Table 1). The MP3/DZP++// MP2/DZP++ method predicts an EA value closer to that reported experimentally (2.718 ± 0.008 eV). One expects the CCSD(T) method to ultimately provide close agreement with experiment, but only when much larger basis sets than DZP++ are used. The greater (than DFT) sensitivity to basis set of convergent quantum mechanical methods is well known. Note that the ZPVE corrected and uncorrected EA values, Table 1, are in good agreement but only the corrected EAs will be discussed in the subsequent text.

Table 2 summarizes the gas-phase basicities and the electronic Gibbs free-energy changes (ΔG_e°, kcal/mol) for the different fluoropropynide anions. Note that the thermally corrected (298.15 K, 1 atm) Gibbs free-energies are reported in parentheses. From Table 2, the gas-phase basicity values decrease with increasing fluorine substitution, clearly showing that the introduction of an electronegative substituent causes the nucleophilicity of the carbanions to decrease, yielding a decrease in basicity. Clearly, the energy gap between the anionic species and its conjugate acid decreases with the number of fluorine atom substituents.

The exothermicity of the fluoropropynl radicals toward $H^{\bullet}$ addition, however, shows an opposite trend as compared to those depicted by the respective anions. Trifluoropropyne shows the greatest endothermicity among the group of fluoropropynes. Note that basicity on going from $H_3C{-}C{\equiv}C{:}^{-}$ to $F_3C{-}C{\equiv}C{:}^{-}$ changes by ca. 30 kcal/mol while the CH bond dissociation energy of

TABLE 2. Gas-Phase Basicities or Absolute Basicities of Fluoropropynyl Anions and Radicals[a]

		Gibbs free energy change, ΔG_e° (kcal/mol)			
methods		$H_3C-C\equiv C:^-$	$FCH_2-C\equiv C:^-$	$F_2CH-C\equiv C:^-$	$F_3C-C\equiv C:^-$
DFT	BHLYP/DZP++	374.3	361.2	351.5	344.4
	BLYP/DZP++	369.7	355.1	345.3	338.9
	B3LYP/DZP++	372.2	358.5	348.7	341.9
	BP86/DZP++	370.6	356.6	347.1	340.7
	BPW91/DZP++	373.1	359.1	349.4	343.0
	B3PW91/DZP++	374.5	361.1	351.5	344.8
ab initio[b]	LCAO−SCF-MO/4-31G	413.8	397.4	382.5	369.3
experiment[c]		373.4 ± 2			

method		$H_3C-C\equiv C^\bullet$	$FCH_2-C\equiv C^\bullet$	$F_2CH-C\equiv C^\bullet$	$F_3C-C\equiv C^\bullet$
DFT	B3LYP/DZP++	135.8 (127.2)	135.9 (127.7)	139.1 (130.7)	140.1 (132.7)

[a] These are thermally corrected ΔG values (298.15 K, 1 atm). Note that for the radicals, basicities also refer to the homolytic bond dissociation energies. [b] Reference 11b. [c] Reference 14.

TABLE 3. Harmonic Vibrational Frequencies (cm^{-1}), IR Intensities (km/mol), and Mode Assignments of the α-Fluoropropynyl Radical and Anion, Predicted by the B3LYP/DZP++ Method

	radical				anion			
vibrational mode	symmetry	frequency	IR intensity	mode assignment	symmetry	frequency	IR intensity	mode assignment
ν_1	A	185	2	C−C≡C twist	A	190	3	C−C≡C bend
ν_2	A	294	31	C−C≡C bend	A	265	2	C−C≡C bend
ν_3	A	511	1	C−C−F bend	A	484	10	C−C−F bend
ν_4	A	870	42	C−C−H bend	A	824	287	C−F stretch
ν_5	A	925	20	C−C stretch	A	975	92	C−C stretch
ν_6	A	1051	206	C−F stretch	A	1003	10	CH_2 wag
ν_7	A	1217	11	CH_2 twist	A	1199	1	CH_2 twist
ν_8	A	1352	67	CH_2 wag	A	1342	88	CH_2 wag
ν_9	A	1417	69	CH_2 scissors	A	1470	6	CH_2 scissors
ν_{10}	A	1643	389	C≡C stretch	A	2040	211	C≡C stretch
ν_{11}	A	3023	24	CH_2 symmetric stretch	A	2980	188	CH_2 symmetric stretch
ν_{12}	A	3967	4	CH_2 antisymmetric stretch	A	3008	83	CH_2 antisymmetric stretch

TABLE 4. Harmonic Vibrational Frequencies (cm^{-1}), IR Intensities (km/mol), and Mode Assignments of the α-Difluoropropynyl Radical and Anion Predicted by the B3LYP/DZP++ Method

	radical				anion			
vibrational mode	symmetry	frequency	IR intensity	mode assignment	symmetry	frequency	IR intensity	mode assignment
ν_1	A″	125	7	C−C≡C twist	A″	164	5	C−C≡C twist
ν_2	A′	209	29	C−C≡C bend	A′	204	3	C−C≡C bend
ν_3	A″	417	9	C−C−F bend	A′	447	1	F−C−F bend
ν_4	A′	457	1	F−C−F bend	A″	496	0	CF_2 deformation (out of phase)
ν_5	A′	617	8	CF_2 deformation (out of phase)	A′	600	14	CF_2 deformation (in phase)
ν_6	A′	874	409	CF_2 deformation (in phase)	A″	889	322	CF_2 antisymmetric stretch
ν_7	A″	1071	190	CF_2 antisymmetric stretch	A′	931	151	CF_2 symmetric stretch
ν_8	A′	1112	345	CF_2 symmetric stretch	A′	1046	347	C−C stretch
ν_9	A′	1326	672	C−H wag (in plane)	A″	1313	13	C−H wag (in plane)
ν_{10}	A″	1345	6	C−H wag (out of plane)	A′	1341	182	C−H wag (out of plane)
ν_{11}	A′	1509	952	C≡C stretch	A′	2060	335	C≡C stretch
ν_{12}	A′	3095	23	C−H stretch	A′	3030	120	C−H stretch

neutral fluoropropynes does not change significantly (only 5 kcal/mol).

H. Vibrational Frequencies. The B3LYP vibrational frequencies and normal mode assignments for the three fluoropropynyl radicals and anions computed are reported in Tables 3−5. The B3LYP harmonic vibrational frequencies associated with the C≡C bond in the four radicals are $CH_3-C\equiv C^\bullet$ (1669 cm^{-1}), $FCH_2-C\equiv C^\bullet$ (1643 cm^{-1}), $F_2CH-C\equiv C^\bullet$ (1509 cm^{-1}), and $CF_3-C\equiv C^\bullet$ (2250 cm^{-1}). Likewise, the B3LYP harmonic vibrational frequencies for the C≡C bond in the anions are $CH_3-C\equiv C:^-$ (2037 cm^{-1}), $FCH_2-C\equiv C:^-$ (2040 cm^{-1}), $F_2CH-C\equiv C:^-$ (2060 cm^{-1}), and $CF_3-C\equiv C:^-$ (2075 cm^{-1}). The fundamental vibrational frequency associated with a C≡C bond is known to lie typically in the range 2000−2500 cm^{-1}.

TABLE 5. Harmonic Vibrational Frequencies (cm^{-1}), IR intensities (km/mol), and Mode Assignments of the α-Trifluoropropynyl Radical and Anion Predicted by the B3LYP/DZP++ Method

	radical				anion			
vibrational mode	symmetry	frequency	IR intensity	mode assignment	symmetry	frequency	IR intensity	mode assignment
ν_1	E	102	5	C−C≡C twist	E	162	5	C−C≡C twist
ν_2	E	102	5	C−C≡C bend	E	162	5	C−C≡C bend
ν_3	E	405	0	C−C−F bend	E	425	0	C−C−F bend
ν_4	E	405	0	CF_3 deformation (out of phase)	E	425	0	CF_3 deformation (out of phase)
ν_5	A_1	541	5	CF_3 deformation (in phase)	A_1	543	5	CF_3 deformation (in phase)
ν_6	E	566	0	C−C−F bend	E	581	0	C−C−F bend
ν_7	E	566	0	C−C−F bend	E	581	0	C−C−F bend
ν_8	A_1	807	17	CF_3 symmetric stretch	A_1	760	17	CF_3 symmetric stretch
ν_9	E	1155	398	CF_3 antisymmetric stretch	E	1001	398	CF_3 antisymmetric stretch
ν_{10}	E	1155	398	C−F stretch	E	1001	398	C−F stretch
ν_{11}	A_1	1228	793	C−C stretch	A_1	1207	793	C−C stretch
ν_{12}	A_1	2250	396	C≡C stretch	A_1	2075	396	C≡C stretch

The low vibrational frequencies seen here for the radicals reflect the weaker C≡C triple bonds. The C−C≡C structures in the radicals are significantly bent (by ca. 20°), with long C≡C distances for the mono- and difluoropropyne (B3LYP method). Accordingly, a lower frequency for these radicals is encountered. As a result, significant double-bond character is expected. Furthermore, the molecular orbital section indicates that the radicals have a singly occupied σ-orbital as opposed to anions, which have completely filled σ as well as π-orbitals. Hence, taken to the extreme, one might hypothesize a vinylidine-like $CH_3-C=C:$ valence structure for the propynyl radical. Also, the natural bond orbital (NBO) analyses predict bond orders of less than three for the radicals, and there is a modest lengthening of the C≡C bond. However, for the perfluorinated $CF_3-C\equiv C^{\bullet}$ radical a higher C≡C frequency (2250 cm^{-1}) is seen, reflecting the C−C≡C linearity. For the anions, the B3LYP method predicts "normal" C≡C harmonic stretching frequencies, and it is observed that the frequencies increase as the F atoms substitute H atoms on the α-CH_3 group.

The predicted C≡C vibrational frequencies show significant variation with the density functional method employed for the computations. We note that the C≡C vibrational frequency varies from 1564 (B3PW91) to 1909 cm^{-1} (BHLYP) and shows no discernible correlation with the C≡C bond length for the monofluoropropynyl radical; this, in general, is true for the other radicals. However, we find that this stretching frequency is noticeably correlated to the C−C≡C bond angle. Functionals that predict a *quasi* linear C−C≡C moiety, generally, show C≡C stretching frequencies close to 2000 cm^{-1}. In contrast, the other functionals, which favor significantly bent C−C≡C structures, have C≡C stretching frequencies in the range of 1600 cm^{-1}. This remarkable inconsistency in the vibrational frequencies for the bent structures is due to the coupling of C≡C stretch with the C−C stretching and C−C−H bending modes. With the C−C≡C bond angle tending toward linearity, the coupling of C≡C with the C−C stretching and C−C−H bending modes is decreased. To further verify this coupling, we have computed the C≡C vibrational frequencies of (forced) linear and bent ethyne radical, C_2H.

SCHEME 1. C≡C Stretching Mode for the Linear and Bent Ethynyl Radical Structures[a]

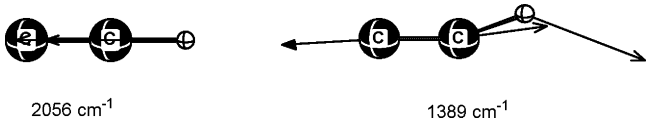

[a] The geometries and the vibrational frequencies were computed at the B3LYP/DZP++ level. Note that the linear ethynyl radical is not a minimum at this level of theory.

The B3LYP/DZP++ C≡C vibrational frequencies for the (constrained) linear and bent structures are 2056 and 1389 cm^{-1}, respectively. The vectors for the respective vibrations for the linear and bent structures displayed in Scheme 1 clearly justify the coupling of the C≡C stretching with the C−C−H bending mode. Note that the changes in the vibrational frequencies at different levels of theory do not refer to the Σ and Π states but are due to coupling of the stretching and bending modes.

I. Molecular Orbitals. Figure 6 shows the SOMOs and the HOMOs at the MP2 optimized geometries of the radicals and their respective anions. The SOMO of the radicals should display the stabilization interaction between the σ electrons and the adjacent singly occupied C≡C π orbital. The qualitative picture of the SOMOs for the various radicals is unchanged with increasing F atom substitution.

For these fluorocarbanions there are two electronic effects, which reinforce each other: (1) four-electron destabilization due to CH_2 groups and (2) the stabilization offered by the favorable interaction of the σ*-orbital associated with the C−F bond with the π-orbital of the C≡C bond. The four-electron (destabilizing) term arises due to electron (two each) contributions from the CH_2 group due to hyperconjugation, and from the anion.[31] The former destabilizing effect is the largest for $FCH_2-C\equiv C:^-$, while the latter stabilizing effect is maximized in $F_3C-C\equiv C:^-$ to such an extent that the π-bonding orbital lies energetically below the σ-bonding orbital. Thus, the anion stabilization increases with successive

(31) Jarowski, P. D.; Wodrich, M. D.; Wannere, C. S.; Schleyer, P. v. R.; Houk, K. N. *J. Am. Chem. Soc.* **2004**, *126*, 15036.

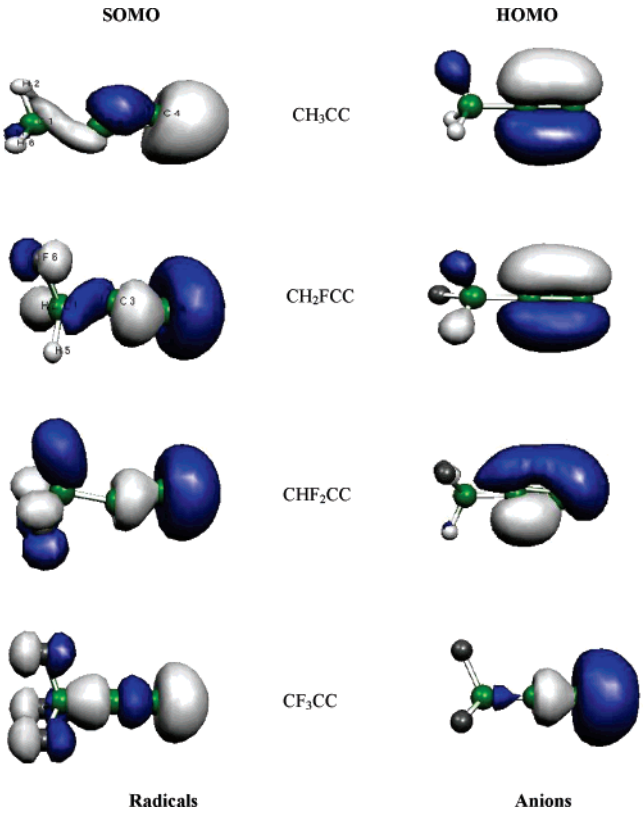

FIGURE 6. Plots of the SOMO and HOMO of the fluorine derivatives of the propynyl radical and anion.

fluorine substitution. Accordingly, the electron affinities increase in the following order: $FCH_2-C\equiv C:^- < F_2CH-C\equiv C:^- < F_3C-C\equiv C:^-$.

J. Fluorine-Substituted Propargyl Radical Isomers, and Their Anions. Also considered in this research were the isomeric propargyl radicals, $^\bullet CR_2-C\equiv CR$. Here the parent propargyl radical, $^\bullet CH_2-C\equiv CH$, is compared (B3LYP/DZP++) with the parent propynyl radical, $CH_3-C\equiv C^\bullet$, and their isomeric fluorine derivatives have also been studied.

(a) Structures of Propargyl Radicals and Anions (Figure 7). Propargyl Radical and Anion (Figure 7; structures **a** and **a′**): At the B3LYP/DZP++ level, the propargyl radical shows a C_{2v} minimum (**a** in Figure 7) while its anion (**a′** in Figure 7), with the C_s symmetry, is bent with C−C−C and C−C−H angles close to 174° and 120°, respectively. The significantly twisted C−C−H angle in **a′** shows that the negative charge is mainly localized at the terminal (C_1) CH group. Note that the intermediate (neither double nor triple) C−C bond distances are indicative of alkenyl structure rather than alkynyl-type structure for the propargyl radical (**a**) and anion (**a′**).

Monofluoropropargyl Radical andAnion (Figure 7; structures **b**, **b′**, **c**, and **c′**): Two isomers exist for the monofluoropropargyl radical and its anion: terminal CF (**b** and **b′**) and terminal CH (**c** and **c′**), Figure 7. The structures with the terminal CH are energetically preferred over the terminal CF isomers. The C−C bond lengths of the monofluoropropargyl radical and anions with terminal CH are remarkably similar to those of the respective parent structures.

The radical isomer with the terminal CH has an almost linear C−C−C moiety while the CF isomer is bent with a C−C−F angle of 147°. In contrast to the radicals, both the isomers of anion are significantly bent with C−C−X (X = F, H) angles of ca. 115°.

Difluoropropargyl Radical and Anion (Figure 7; structures **d**, **d′**, **e**, and **e′**): Similar to the monofluoropropargyl analogues, the difluoropropargyl radical and its anion have two isomers; the terminal CH stucture is energetically preferred. The CH radical isomer has a C_{2v} minimum while the respective anion favors a C_s structure. The intermediate C−C bond lengths in all the isomers are indicative of alkenyl-type structures.

Trifluoropropargyl Radical and Anion (Figure 7; structures **f** and **f′**): Trifluoropropargyl radical and anion (**f** and **f′**) both have bent structures. The radical has a $^2A'$ ground state. The C2−C1−F4 bond angle in the trifluropropargyl anion deviates much more from linearity (111.5°) than that for the radical (138.6°). The CC bond lengths in trifluoropropargyl and the propargyl radical (and their respective anions) are remarkably different. The nearly equal CC bond lengths in the trifluoropropargyl anion indicate a delocalized negative charge.

(b) Relative Energies of the Radicals. The electronic energies of the propynyl and propargyl radicals are presented in Table 6. The parent propargyl radical (B3LYP/DZP++) is predicted to lie 40.6 kcal/mol below the propynyl radical. The stability of the propargyl radical relative to the propynyl radical lies in the fact that the allenyl system is stabilized by the four-electron interactions of the two C−H σ-bonds. The monofluoropropargyl radicals ($^\bullet CH_2C\equiv CF$ and $^\bullet CHFC\equiv CH$) are also predicted to lie lower in energy than the α-fluoropropynyl radical ($CH_2FC\equiv C^\bullet$), by 30.6 and 43.7 kcal/mol, respectively. The stability of these monosubstituted fluoro compounds is governed by hyperconjugation with the C−F nonbonding electrons. However, in the $^\bullet CH_2C\equiv CF$ radical, the degree of hyperconjugation is less than for the $^\bullet CHFC\equiv CH$ radical.

Among the difluoro systems, it is predicted that the $^\bullet CF_2-C\equiv CH$ propargyl radical lies lowest in energy, 13.0 kcal/mol below the $^\bullet CHF-C\equiv CF$ radical. The energy difference between the $^\bullet CF_2-C\equiv CH$ and the $HCF_2-C\equiv C^\bullet$ radicals is observed to decrease slightly compared to that of the monofluoro radicals (Table 6). For the trifluoro systems, there are only two isomers, and the propargyl structure $^\bullet CF_2-C\equiv CF$ is predicted to lie 23.5 kcal/mol below that of the α-trifluoropropynyl radical, $CF_3-C\equiv C^\bullet$. Note that for the parent, mono-, and difluorinated derivatives the energy difference between the propargyl and propynyl radicals is very large (ca. 40 kcal/mol). In sharp contrast, this energy difference in the respective propargyl and propynyl anions is negligible, indicating that the substitution of H by F has a noticeable difference on the stability of the propynyl derivatives.

(c) Relative Energies of the Anions. The relative energies of the anion systems are very different from those of the radicals (Table 7). A tiny energy difference between the propynyl anion and the propargyl anion (0.1 kcal/mol) is predicted by the B3LYP/DZP++ method. In the monofluoro systems, it is predicted that the α-fluoropropynyl anion lies energetically below the two monofluoropropargyl anions. The $FCH_2-C\equiv C:^-$ anion is 6.2

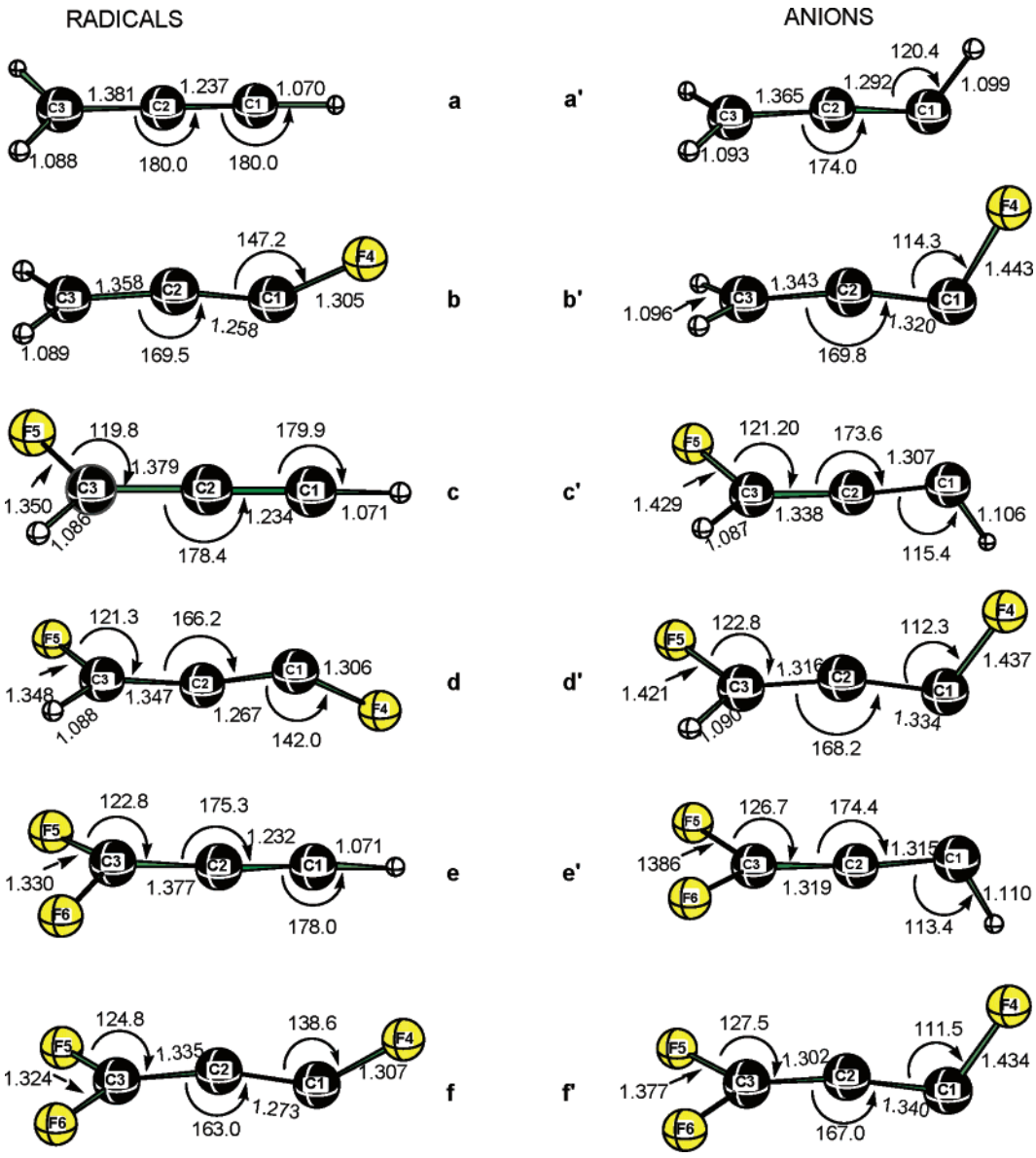

FIGURE 7. B3LYP/DZP++ optimized geometries of the propargyl radical and anion and the fluoropropargyl radicals and anions.

TABLE 6. Relative Energies of the Radicals and Anions

radicals	relative energy (kcal/mol)	anions	relative energy (kcal/mol)
$CH_3C{\equiv}C^{\bullet}$	40.6	$CH_3C{\equiv}C{:}^-$	0.1
$^{\bullet}CH_2C{\equiv}CH$	0	$^-{:}CH_2C{\equiv}CH$	0
$CH_2FC{\equiv}C^{\bullet}$	43.7	$^-{:}CH_2C{\equiv}CF$	6.9
$^{\bullet}CH_2C{\equiv}CF$	13.1	$^-{:}CHFC{\equiv}CH$	6.2
$^{\bullet}CHFC{\equiv}CH$	0	$CH_2FC{\equiv}C{:}^-$	0
$HCF_2C{\equiv}C^{\bullet}$	42.3	$^-{:}CF_2C{\equiv}CH$	17.2
$^{\bullet}CHFC{\equiv}CF$	13.0	$^-{:}\,CHFC{\equiv}CF$	14.0
$^{\bullet}CF_2C{\equiv}CH$	0	$HCF_2C{\equiv}C{:}^-$	0.0
$CF_3C{\equiv}C^{\bullet}$	23.5	$^-{:}CF_2C{\equiv}CF$	23.4
$^{\bullet}CF_2C{\equiv}CF$	0	$CF_3C{\equiv}C{:}^-$	0

TABLE 7. Electron Affinities of Fluorine Derivatives of the Propargyl Radical Computed with the B3LYP/DZP++ Method[a]

	radical symmetry state	anion symmetry state	electron affinity (eV)
$CH_2C{\equiv}CH$	$C_{2v}\,^2B_1$	$C_s\,^1A'$	0.97 (0.98)
$CHFC{\equiv}CH$	$C_s\,^2A''$	$C_1\,^1A$	1.16 (1.18)
$CF_2C{\equiv}CH$	$C_1\,^2A$	$C_s\,^1A'$	1.30 (1.32)
$CH_2C{\equiv}CF$	$C_s\,^2A'$	$C_s\,^1A'$	1.69 (1.71)
$CHFC{\equiv}CF$	$C_1\,^2A$	$C_1\,^1A$	2.01 (2.05)
$CF_2C{\equiv}CF$	$C_s\,^2A'$	$C_s\,^1A'$	2.18 (2.23)

[a] Zero-point vibrationally corrected EAs are in parentheses.

kcal/mol below the $^-{:}CHF{-}C{\equiv}CH$ anion, while the latter is only 0.7 kcal/mol below its isomer, $^-{:}CH_2{-}C{\equiv}CF$.

Similarly, the α-difluoropropynyl anion is predicted to be more stable than the two difluoropropargyl anions. The $HCF_2{-}C{\equiv}C{:}^-$ anion is found to lie 14.0 kcal/mol below the $^-{:}CFH{-}C{\equiv}CF$ anion, and the latter is 3.2 kcal/mol below the isomeric $^-{:}CF_2{-}C{\equiv}CH$ anion. Finally, the α-trifluoropropynyl anion, $CF_3{-}C{\equiv}C{:}^-$, is predicted to lie 23.4 kcal/mol below the trifluoropropargyl anion, $^-{:}CF_2{-}C{\equiv}CF$.

In general, it is observed that the fluoropropynyl anions lie lower in energy than the analogous fluoropropargyl anions. This conclusion requires that the addition

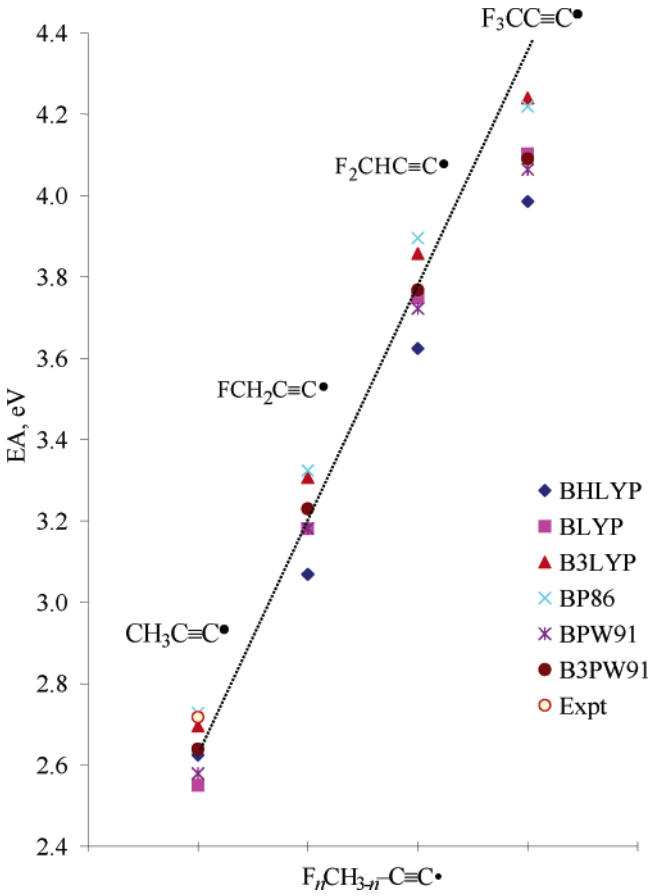

FIGURE 8. Electron affinities of the different fluoropropynyl radicals computed at various levels of theory with the DZP++ basis set.

of an electron to the fluoropropynyl radicals is much more exothermic than is the case for the fluoropropargyl radicals.

(d) Electron Affinities of the Propargyl Radical and Its Fluorine-Substituted Species. Propargyl radicals show much smaller electron affinities than those of the isomeric fluoropropynyl radicals. The electron affinity of the propargyl radical ($^\bullet CH_2{-}C{\equiv}CH$, C_{2v} $^2B_1$) was predicted earlier by Rienstra-Kiracofe and coworkers.[29] The B3LYP/DZP++ electron affinity of the propargyl radical (0.98 eV) was found to be closest to experiment (0.918 ± 0.008 eV) compared to other functionals. The electron affinities (B3LYP/DZP++) of the fluorinated propargyl radicals, $^\bullet CHF{-}C{\equiv}CH$, $^\bullet CF_2{-}C{\equiv}CH$, $^\bullet CH_2{-}C{\equiv}CF$, $^\bullet CHF{-}C{\equiv}CF$, and $^\bullet CF_2{-}C{\equiv}CF$, are presented in Table 7. The nearly linear plot of EA versus number of fluorine substituents (Figure 8) is not anticipated, but nevertheless is interesting. Analogous plots for other thermochemical quantities such as proton affinities do not follow straight lines.

It is predicted that the introduction of an electronegative fluorine atom in the propargyl system causes the electron affinities to increase monotonically. The parent propargyl radical, $^\bullet CH_2C{\equiv}CH$, has a much lower EA value (0.98 eV) than $^\bullet CH_2C{\equiv}CF$ (1.71 eV). The monofluorinated propargyl isomer, the $^\bullet CHF{-}C{\equiv}CH$ radical, has a lower electron affinity (1.18 eV). Recall that $FCH_2{-}C{\equiv}C^\bullet$ (Table 1) has a much higher electron affinity (3.31 eV). The presence of the fluorine at the α-C atom

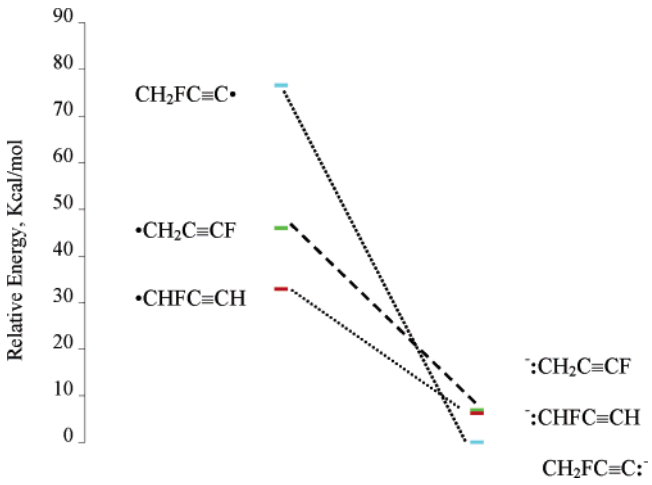

FIGURE 9. Relative energies of monofluoro propargyl and propynyl radicals and anions computed at the B3LYP/DZP++ level.

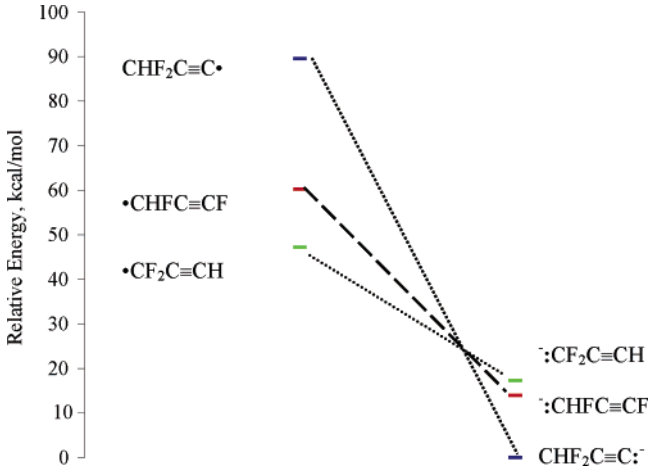

FIGURE 10. Relative energies of difluoro propargyl and propynyl radicals and anions computed at the B3LYP/DZP++ level.

in the $^\bullet CHF{-}C{\equiv}CH$ radical causes stabilization due to negative hyperconjugation, and this further decreases the energy gap between the radical and its anion. However, there is also electronic destabilization in the $^\bullet CH_2{-}C{\equiv}CF$ radical due to the influence of the C–H σ-bonding electrons (compare radical energies in Table 7).

The difluoro $^\bullet CF_2{-}C{\equiv}CH$ radical is predicted to have a lower electron affinity (1.32 eV) than its isomer, $^\bullet CHF{-}C{\equiv}CF$ (2.05 eV). Both, of course, show much smaller electron affinities than $F_2CH{-}C{\equiv}C^\bullet$ (3.86 eV). There is a significant increase in the electron affinity of the perfluorinated radical $^\bullet CF_2{-}C{\equiv}CF$ (2.23 eV) compared to $^\bullet CH_2{-}C{\equiv}CH$ (0.98 eV). However, the perfluoro $F_3C{-}C{\equiv}C^\bullet$ radical (4.22 eV) still has a much higher electron affinity (Table 1).

IV. Concluding Remarks

Simple fluoroalkynyl radicals show significant contrasts with their isomeric fluoroallenyl species. In this research, propynyl radicals and anions have been com-

pared with propargyl radicals and anions. Compared to the parent molecules, the fluorine derivatives are shown to exhibit important changes in their structures and energetics. Specifically, the geometries, electron affinities, and gas-phase basicities are predicted to change radically as a function of the number of fluorine substituents.

The energetic predictions from the present research are most easily appreciated in Figures 9 and 10. Figure 9 shows that the energetic ordering of the monofluoro propynyl and propargyl radicals switches upon addition of an electron. The same effect is seen for the difluoro radicals and anions in Figure 10. What a difference an electron makes!

Acknowledgment. The authors thank Francesco A. Evangelista and Brian N. Papas for helpful discussions. R.K.S. thanks the Tertiary Education Commission (TEC), Mauritius, and the Center for Computational Chemistry for encouraging the completion of this work. This research has been supported by the U.S. Department of Energy Combustion Research program.

Supporting Information Available: Cartesian coordinates and harmonic vibrational frequencies predicted by the MP2 and DFT methods with the DZP++ basis sets for all the structures. This material is available free of charge via the Internet at the http://pubs.acs.org.

JO0507688